

The extensive development of practical applications of different electron-beam technologies is associated with the problem of electron beam transport over significant distances. As a rule, the transport of quasineutral electron beams along a magnetic field is utilized here.

During the practical realization researchers encounter the origination of a broad spectrum of different instabilities inhibiting the effective transmission of beam energy to the target. Instabilities are ordinarily of threshold nature and appear when the beam current exceeds the limit value. Such an approach to analysis of the instabilities is proposed in [1], where different aperiodic instabilities of the pierce, beam-drift type resulting in beam destruction are examined in detail. The case of strong magnetic fields was investigated experimentally, when the beam-drift instability threshold is above the limit vacuum current. The opposite case of weak magnetic fields was not investigated. The domain of such magnetic fields and energies is studied in this paper when the beam-drift instability current is less than the vacuum current. An instability is developed for currents less than the vacuum values that is manifested by the fact that amplitude-inhomogeneous current density fluctuations occur in the beam at a frequency close to the ionic Langmuir frequency. No detailed investigation of these fluctuations has been performed earlier. Meanwhile it is evident that a study of the beam state and evolution in the prelimiting modes permits not only a better comprehension of the collapses for currents higher than the vacuum values but their determination and prevention in advance.

An attempt is made in this paper to give a physical interpretation of the occurring instability and to answer the following questions: does the beam remain compensated upon appearance of the fluctuations as the deformation of its structure occurs, and what are the criteria for instability origination and stabilization? A qualitative model of the instability is presented that satisfactorily agrees with experimental observations.

EXPERIMENTAL INSTALLATION AND METHODOLOGY

The diagram of the experimental installation is shown in Fig. 1. A three-electrode gun consisting of a lanthanum hexaboride cathode of \varnothing 10 mm of indirect heating 1, an anode grid 2, and a preaccelerating electrode 3, was used to shape the beam. The latter is needed to prevent the origination of a virtual cathode near the anode grid [2], which was achieved by delivery of a positive or even small negative bias to it by using the source 4. The total electron energy in the experiments was approximately 4 keV and was given by the source 5. The beam current was regulated by a voltage pulse U_y that came from the source 6. The synchronization was such that at the time of the pulse the cathode heating spiral current was zero. The pulse duration could be regulated between 10 and 300 μ sec. The current working band was from 50 mA to 1 A.

The \varnothing 10 cm and 3.3 m long drift tube 7 was evacuated to the pressure $p = 2.7 \cdot 10^{-4} - 1.3 \cdot 10^{-2}$ Pa and the working gas was air. The magnetic field was produced by the coils 8. Its magnitude was regulated to 400 Oe. The beam was taken at the graphite collector 9 or on a special target 10 from stainless steel covered by a k-80 luminophor and disposed at an angle close to 45° to the drift tube axis. The glow caused by the beam by using an electrooptic converter (EOC) 11 could be photographed through the viewing window. In the experiments the collector (or luminophor target) was electrically connected to the preaccelerating electrode, consequently, the voltage on it was also regulated by the source to +300 V.

The following methodology was used in the experiments. The capacitive probe 12 was intended to measure the beam linear charge. It was a cylindrical grid mounted in the middle part of the drift tube. A wire probe 13 was used to measure the current density and beam

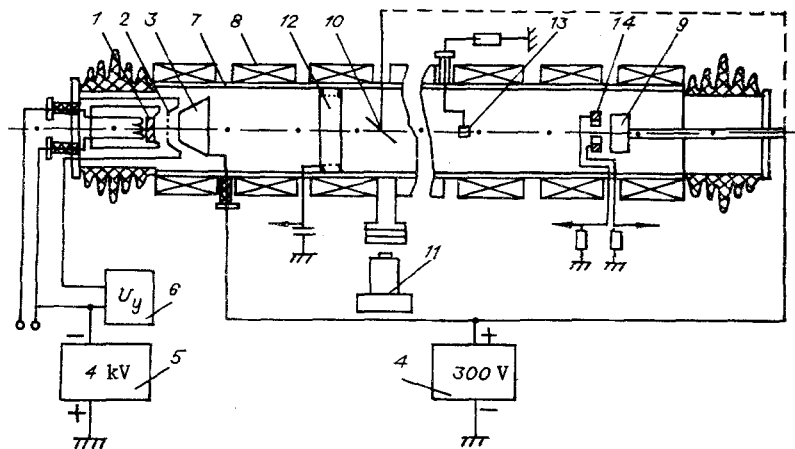


Fig. 1

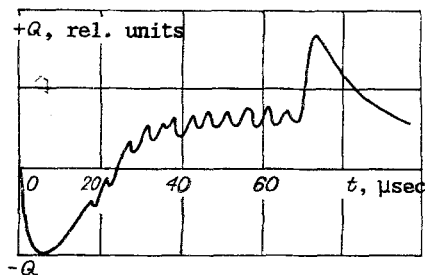


Fig. 2

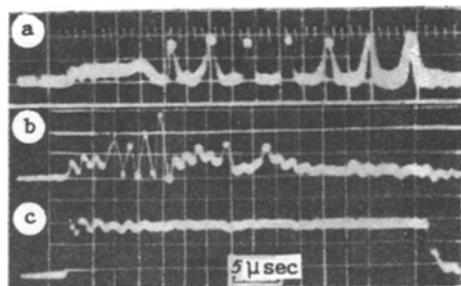


Fig. 3

potential. The working part of the probe is a tungsten cylinder of \varnothing 3 mm and altitude 3 mm. Potential measurements were performed when the probe was within the beam limits, and are based on the secondary emission phenomenon. Upon delivery of positive bias the number of secondary electrons leaving the probe starts to diminish, and therefore, the total current coming in to the probe should increase when the probe potential becomes somewhat higher than the beam potential. These measurements did not have the aim of giving the exact magnitude of the potential but were utilized for a qualitative estimate: the beam is positive or negative relative to the tube walls.

The luminophor target with the EOC permitted photographing the "visualized" beam structure at different times. The exposure was 1 μ sec, and the luminophor afterglow was less than 1 μ sec. The pickup electrodes 14 were two halves of a cylinder of \varnothing 3 cm and altitude 3 cm, mounted insulated ahead of the collector. The current going to it could be determined.

RESULTS OF THE EXPERIMENTS

In order to avoid secondary electron accumulation in the beam and the origination of different plasma instabilities, a positive potential was delivered to the collector (and to the preaccelerating electrode). This created the possibility of secondary electron entrainment in the longitudinal direction and the formation of a two-component plasma. To do this it is necessary that the condition

$$n_2/n_1 \ll L/(\langle v \rangle \tau_i),$$

be satisfied, where n_2 is the secondary electron concentration, n_1 is the beam electron concentration, L is the drift tube length, τ_i is the ionization time, and $\langle v \rangle$ is the mean velocity of the secondary electrons.

The ionization time was measured by using a capacitive probe whose signal diminished linearly with time upon the connection of the current. The slope of the oscillogram governed the value of τ_i which diminished in inverse proportion to the pressure and was independent of the magnetic field. For a 4 keV energy $\tau_i \approx 45 \mu$ sec for $p = 2.7 \cdot 10^{-4}$ Pa. If we take $\langle v \rangle \approx 3 \cdot 10^8$ cm/sec, then the ratio n_2/n_1 will equal unity for $p = 1.2 \cdot 10^{-3}$ Pa for $L = 3 \cdot 10^2$ cm, i.e., the plasma is practically two-component at the working pressures.

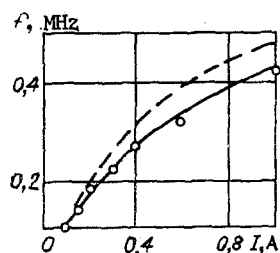


Fig. 4

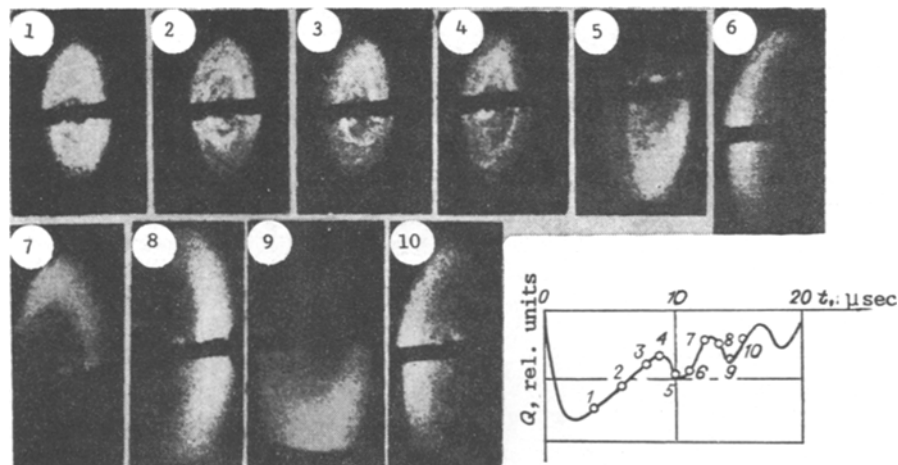


Fig. 5

It is clarified as a result of the experiments that the fluctuations occurred for sufficiently high currents and were recorded by the methods listed above. Let us examine each of them in greater detail.

A typical oscillogram of the capacitive probe is presented in Fig. 2. Fluctuations do not occur at once but after a certain time, somewhat less than the ionization time, when the beam linear charge is still not completely compensated by the ions. Then the signal at the probe changes sign, becoming positive. Special measurements showed that the signal becomes positive because of charging of the problem by the ion current rather than because of "beam overcompensation."

Fluctuations with the same frequency were recorded by the wire probe when it was placed in beams or was located in direct proximity to the beam edge. A typical oscillogram is presented in Fig. 3 (a is the wire probe oscillogram for $p = 9.7 \cdot 10^{-4}$ Pa, b is the same for $p = 4.6 \cdot 10^{-3}$ Pa, c is the 200 mA collector current, and the pulse duration is 40 μ sec). The fluctuations appear at the same time and with the same frequency as on the capacitive probe. When the wire probe is located outside the beam, 100% modulation was observed. The fluctuation frequency did not depend on the pressure in the range $p = 2.7 \cdot 10^{-4} - 1.3 \cdot 10^{-3}$ Pa and the magnetic field intensity as it varied between 100 and 400 Oe. The dependence of the fluctuation frequency on the current is presented in Fig. 4. It is seen that the frequency varies approximately as \sqrt{I} . The dependence $\sim\sqrt{I}$ is shown by dashed lines.

Fluctuations with the same frequency were observed at the pickup-electrodes, where the signals on them were shifted 180° in phase. This permitted making the deduction that the fluctuations are amplitude-inhomogeneous and that a beam having an inhomogeneous current density rotates in time around an axis with the frequency observed. As the magnetic field diminishes, the signal amplitude at the pickup-electrodes increased practically linearly.

Photographs of the luminophor target by using the EOC yielded the most graphic information about the beam structure and motion in an unstable state. A series of such photographs and oscillograms of the capacitive probe is represented in Fig. 5, the exposure times of the appropriate frames are marked with circles. At the initial times (up to frame 4) the beam has a homogeneous structure. The beginning of the fluctuations agrees with the formation of

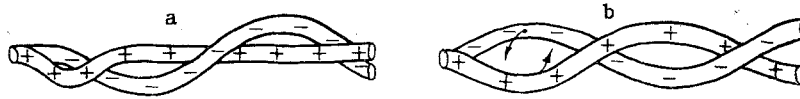


Fig. 6

an inhomogeneous current density in azimuth (frames 4-6). Then this inhomogeneity is displaced clockwise, which corresponds to electron rotation in a given magnetic field. The photographs show that the beam structure becomes acutely inhomogeneous during the fluctuations and acquires the form of half-moons that rotates around the axis.

Let us note that the distance between the gun and the luminophor target was 1.3 m, and to the collector 3.3 m. Other conditions being equal, no changes were here detected in the fluctuation frequency.

QUALITATIVE THEORY AND CONTROL EXPERIMENTS

Experiments showed that the fluctuations observed are a result of beam rotation as a whole around the drift tube axis. This affords a foundation for assuming that under such a rotation the beam charges and ions are separated. On this basis let us try to describe qualitatively the processes to which such a charge distribution leads.

Let us first note that it is sufficient to assume that separation occurred locally rather than on the whole beam length since a local perturbation is propagated over the whole length (Fig. 6a) because of electron drift in $E \times H$ fields. If the ions were to remain fixed here, then a stationary beam shift relative to its location in the unperturbed state would be observed in some plane perpendicular to the beam axis. Indeed the ions will be displaced in the beam direction. This will result in the perturbed field becoming diminished whereupon the electrons would be shifted in an azimuthal direction that is opposite to the drift velocity and agrees with the direction of Langmuir electron rotation. In turn, the ions will also acquire an azimuthal velocity because of the azimuthal beam displacement. Therefore, because of ion motion two spirals are formed, ionic and electron (Fig. 6b) wound around each other and performing a rigid rotation towards Langmuir electron motion. Such a rotating spiral visibility generally characterizes the fluctuational ion motion in an electron beam which is propagated in an external magnetic field.

Let us now examine the dynamics of the ions being generated in the beam by considering that the secondary electrons go off to the positive collector with sufficient rapidity. The ions being formed in the beam have a zero azimuthal velocity and are within its limits until (partially neutralizing the negative charge) the beam is displaced in the azimuthal direction to a sufficient degree, i.e., the beam being rotated leaves behind "a cloud of new" ions, which being incident in an azimuthal field, will evidently pick up the azimuthal velocity and, therefore, be grouped with the already available ions. This means that rotation of a double spiral can last long because of the new ions being formed.

The frequency of spiral rotation can be estimated from the balance equation for the radial forces acting on the ions. In the general case the nonrelativistic equation of particle motion in an electromagnetic field will be written in the form

$$\frac{\partial \mathbf{v}}{\partial t} + (\mathbf{v} \nabla) \mathbf{v} = \frac{e}{m} \mathbf{E} + \frac{e}{mc} [\mathbf{v} \mathbf{H}], \quad (1)$$

where \mathbf{v} , e , m are the particle velocity, charge, and mass, \mathbf{E} , \mathbf{H} are the electrical and magnetic fields, and c is the speed of light. Since rotation occurs stationarily, we shall consider that $\partial \mathbf{v} / \partial t = 0$. Moreover, we omit terms containing the radial component of the ion velocity and the intrinsic magnetic field of the beam. In this case the radial projection of (1) appears as follows

$$-\omega^2 r_i = -\eta_+ E_r + \omega \omega_{ci} r_i. \quad (2)$$

Here r_i , η_+ are the orbit radius and the specific charge of the ion, ω is the frequency of rotation, ω_{ci} is the ion cyclotron frequency, E_r is the radial electrical field (directed towards the system axis). This equation reflects the balance of the centrifugal electrostatic and Lorentz forces acting on the ions. To estimate ω we take the radial electrical field $E_r = E_0(1 - f)$ (E_0 is the radial electrical field on the edge of the decompensated

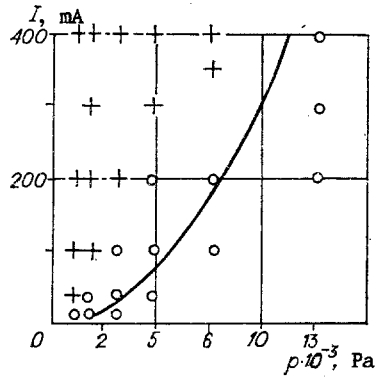


Fig. 7

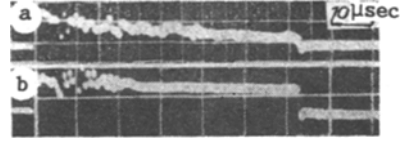


Fig. 8

beam in the unperturbed state, and f is the degree of beam neutralization by the ions being generated). The value of f is determined by the time T during which the beam is shifted by the magnitude of its angular width (we take it equal to $\pi/2$, which is in good agreement with experiment). In this case $T = \pi/(2\omega)$ and therefore $f = \pi/(2\omega\tau_i)$. Introducing the notation $\eta_+ E_0 = (\omega_{pi}^2 r_0)/2$ and solving (2) for ω , we obtain

$$\omega = \frac{\omega_{ci}}{2} \left[\pm \sqrt{1 + \frac{2\omega_{pi}^2 r_0}{\omega_{ci}^2 r_i} \left(1 - \frac{\pi}{2\omega\tau_i}\right)} - 1 \right]. \quad (3)$$

Since rotation occurs towards Langmuir motion, the + sign should be taken in front of the radical in (3).

For $2\omega_{pi}^2 \gg \omega_{ci}^2$ (this condition was satisfied in experiments) (3) is converted into

$$\omega = \frac{\omega_{pi}}{\sqrt{2}} \sqrt{\frac{r_0}{r_i} \left(1 - \frac{\pi}{2\omega\tau_i}\right)}. \quad (4)$$

There hence results that a limit ionization frequency ν_{imax} ($\nu_i = \tau_i^{-1}$) exists for which, when exceeded, the condition for balance of the radial forces (2) cannot be satisfied, therefore, stationary ion rotation becomes impossible. The value of ν_{imax} is determined by the relationship

$$\nu_{imax} = \frac{2\sqrt{2}}{3\pi\sqrt{3}} \sqrt{\frac{r_0}{r_i}} \omega_{pi}. \quad (5)$$

In other words, (5) is the stabilization criterion for this kind of instability that allows of a simple physical interpretation: if $\nu_i > \nu_{imax}$, then any separation of beam charges and ions that occurs will seem to be (in a time less than the period of ion fluctuation) compensated instantaneously by the ions formed by the beam. Under such conditions, the fluctuation nature of ion motion is generally impossible.

The condition $\nu_i < \nu_{imax}$ was satisfied in the experiments described above. The frequency of the fluctuations observed was approximately three times less than $\omega_{pi}/\sqrt{2}$, which agrees sufficiently well with the estimate (4).

Therefore, this instability model explained the beam rotation in time and the rotation frequency. The instability stabilization criterion as p increases results logically from this model.

Control experiments were carried out to verify the criterion (5).

The current in the wire probe was used as instability indicator. As the pressure rose to a certain critical value the oscillograms changed slightly and had the form displayed in Fig. 3a. Then an abrupt change in the oscillogram shape occurred (Fig. 3b). In this case the fluctuations were observed only in the initial instants of the current pulse for $p = 4.6 \cdot 10^{-3}$ Pa. Comparison of these oscillograms permits the statement that stabilization of the instability occurs for $p = 4.6 \cdot 10^{-3}$ Pa.

Results of experiments for different currents and pressures in the drift tube are represented in Fig. 7: the crosses are modes for which instability is observed, and circles for instability stabilized. As the current increases the pressure at which stabilization occurs arises. This is in good agreement with the criterion (5) from which it follows that a definite critical current I^* exists for which instability develops when it is exceeded. If we set $r_1 = r_0$, then we obtain from (5)

$$I^* = \frac{27\pi^2 r_0^2}{32} \frac{v_z}{\eta_+} v_i^2. \quad (6)$$

The dependence (6) is plotted by the line in Fig. 7. The experimental value was taken as v_i . The quantitative discrepancy between theory and experiment is visibly caused by the simplification of the model, consequently, the agreement can be considered completely satisfactory.

Since the model examined is based on the fact that the charges are separated, which means that the beam should have a negative potential, qualitative measurements of the beam potential by the wire probe are carried out for the confirmation. It turns out that when the beam is unstable, the current going to the probe is independent of the delivery of a positive bias thereto and has a shape similar to Fig. 3a. Therefore, the beam indeed has a negative potential, which confirms the assumption made. When stabilization of the instability occurred, the current at the probe increased upon delivery of a positive bias thereto (Fig. 8, where a is the bias $\Delta U = 0$ at the probe, and b for a bias $\Delta U = +80$ V). This permits the conclusion that the beam potential is positive in the stable state. The ion departure mechanisms in the positive and negative beam potential cases are different. For a positive potential the ions depart to the tube wall because of the action of the excess positive ion charge, and for a negative potential leave the beam because of its rotation (in other words, the "beam leaves ions").

Therefore, experiments and the qualitative theory showed that the instability being studied is a beam rotation as a whole around the drift tube axis. The beam charge is here not compensated completely and has a negative magnitude. Evidently, there is a foundation to assume that the rotation, and therefore, the incomplete compensation will be conserved even in the case when the beam current exceeds the vacuum current. The possibility of "undercompensation" was not taken into account in the limit current investigations in [1]. Experimental values were compared with theoretical for completely compensated beams. Their significant divergence is possibly indeed explained by this in certain cases.

The physical model of the instability according to which the beam ions and electrons for two spirals wound around each other and rotating rigidly in the "electron side" is explained well by the results of experiments. Rotation must be taken into account in physical investigations as well as in the design of different devices. Where stable transport is required, it is therefore necessary to select the beam parameters according to the criterion (5) or (6).

Let us note that no fluctuations were detected in [3] for $p < 1.3 \cdot 10^{-6} - 1.3 \cdot 10^{-5}$ Pa, despite attempts to initiate them by using external modulation. The authors associated this with the negligibly small second electron concentration in the beam at such pressures. Secondary electrons are not required in the model taken in this paper. The instability criterion is periodic ion motion in the beam potential well, which is evidently realized at arbitrarily low pressures. When the ion motion becomes aperiodic (at elevated pressure) the instability is stabilized. Additional investigations are apparently needed to resolve this contradiction.

In conclusion, the authors are grateful to A. V. Zharinov for useful discussions and to E. P. Voronkov for equipping the experimental apparatus for operation.

LITERATURE CITED

1. N. V. Nezhlin, Dynamics of Beams in a Plasma [in Russian], Énergoizdat, Moscow (1982).
2. V. A. Malafaev and A. A. Nikul'shina, "Virtual cathode formation in a cylindrical beam," in: 5th All-Union Sympos. in Heavy-Current Electronics: Abstracts of Reports [in Russian], Pt. 1, Tomsk (1984).
3. V. I. Kudelainen, V. V. Pakhromchuk, and D. V. Pestrikov, "Experimental study of the stability of a compensated electron beam," Zh. Tekh. Fiz., 53, No. 5 (1983).